

Submitted, accepted and published in *Fuel Processing Technologies*, 2019 (191)  
111-120; DOI: 10.1016/j.fuproc.2019.04.008

**Towards a sustainable bio-fuels production from lignocellulosic bio-oils: Influence of operating conditions on the hydrodeoxygenation of guaiacol over a Mo<sub>2</sub>C/CNF catalyst**

Javier Remón, Elba Ochoa, Carlos Foguet, José Luis Pinilla\*, Isabel Suelves

Instituto de Carboquímica, CSIC. C/Miguel Luesma Castán 4, 50018 Zaragoza, Spain.

\*Corresponding author: jlpinilla@icb.csic.es

**Abstract:**

This work firstly provides a thorough insight into the effects of the operating conditions (catalyst loading, initial H<sub>2</sub> pressure temperature, reaction time, H<sub>2</sub>/guaiacol ratio and liquid reaction volume) on the hydrodeoxygenation (HDO) of guaiacol over a Mo<sub>2</sub>C/CNF catalyst. Under the operating condition tested, gas and solid formation was negligible and guaiacol was primary converted to different liquid products, including non-deoxygenated (0-oxy), mono-deoxygenated (1-oxy) and fully deoxygenated (2-oxy) compounds, together with high molecular weight soluble oligomers. An increase in the catalyst loading increased the guaiacol conversion and HDO efficiency, augmenting the proportions of HDO products. Among these species, the progressive transformation of 1-oxy compounds into 2-oxy species was kinetically and thermodynamically controlled by the catalyst loading and the amount of H<sub>2</sub> dissolved in the liquid medium, respectively. Augmenting the H<sub>2</sub> pressure increased the H<sub>2</sub> availability in the liquid, which led to increases over time in the guaiacol conversion and HDO efficiency, thus promoting the production of HDO products and facilitating the transformation of guaiacol into fully de-oxygenated products. This increase depended on the reaction volume, with more pronounced variations occurring for a

35 small than for a large volume due to the greater variations occurring in the H<sub>2</sub>/guaiacol  
36 ratio for the former than the latter. The temperature exerted a kinetic promoting effect  
37 together with a thermodynamic inhibitory influence, as some of the reactions involved  
38 were not thermodynamically favoured at high temperature. Therefore, the detailed  
39 analysis included in this work brings novel information on guaiacol HDO, which can  
40 help to establish the basis for catalysts development and reactors design to achieve a  
41 sustainable bio-fuels production from lignocellulosic bio-oils.

42  
43 **Keywords:** guaiacol, bio-oil, bio-fuels, hydrodeoxygenation, Mo<sub>2</sub>C/CNF catalysts  
44  
45

## 46 **1. Introduction**

47 As a result of the world new policies to decrease the current over dependency of crude  
48 oil and mitigate environmental pollution, a lot of effort has been devoted to seeking new  
49 processes, renewable materials and sustainable strategies to produce fuels and chemicals  
50 [1]. As part of this, the use of lignocellulosic biomass to produce these commodities is  
51 gaining increasing attention [2]; hydrothermal liquefaction and fast pyrolysis being  
52 regarded as two promising processes to this end, as they allow the transformation of  
53 biomass into a liquid-energy carrier called bio-oil [3-6].

54  
55 Bio-oil is a dark brown liquid with a higher energy density than the original biomass  
56 [7], it is easy to transport and store, has a relatively high calorific value (HHV around  
57 17 MJ/kg) [8-10] and offers several environmental advantages over fossil fuels [11-13].  
58 However, the high oxygen content and elevated viscosity, acidity and corrosiveness of  
59 bio-oil hinder its use as a liquid biofuel [14] and some upgrading treatments such as  
60 hydrodeoxygenation, hydrocracking, hydrotreating [10] and/or the use of supercritical  
61 water [8, 11-13, 15] are necessary. Among these, hydrodeoxygenation (HDO) is

62 considered an up-and-coming methodology to improve the physicochemical properties  
63 of bio-oils [16]. This process consists of the total or partial removal of the bio-oil  
64 oxygen content under a hydrogen atmosphere at moderate temperature (250-450 °C) and  
65 elevated pressure (40-100 bar) in the presence of a hydrogenation catalyst [17].

66

67 The catalysts generally used for HDO include conventional metal-sulphide  
68 hydrotreating catalysts (NiMoS and CoMoS) [18] as well as noble (Rh, Pt, Pd and Ru)  
69 and transition (Ni, Cu and W) metal supported catalysts [19]. However, these catalysts  
70 have some disadvantages when used for HDO reactions. In particular, metal-sulphides  
71 suffer from deactivation as the sulphur content of the catalyst can be replaced by  
72 oxygen during the HDO reaction, noble metal catalysts require high hydrogen pressures  
73 and may deactivate in the presence of water at high temperatures, while transition  
74 metals deactivate by coking and may also leach to the solution. The supports for these  
75 catalysts include metal oxides ( $\text{Al}_2\text{O}_3$ ,  $\text{SiO}_2$ ,  $\text{ZrO}_2$ ,  $\text{CeO}_2$  and  $\text{TiO}_2$ ), zeolites (HZSM-5)  
76 and carbon-based materials.  $\text{Al}_2\text{O}_3$  is the most widely used support, although it can be  
77 transformed into bohemite at common HDO conditions and its high acidity promotes  
78 the development of side reactions leading to catalyst deactivation [20-22]. Alternative  
79 oxide supports ( $\text{SiO}_2$ ,  $\text{ZrO}_2$ ,  $\text{CeO}_2$  and  $\text{TiO}_2$ ) might be also a plausible option, even  
80 though they are more expensive and have low surface area, while Zeolites are quite  
81 acidic and can only be used at relatively low temperatures [20-22].

82

83 Aiming to overcome these drawbacks, the development of novel, active and resistant  
84 catalysts is gaining increasing attention. On this subject, metal-carbides are regarded as  
85 suitable catalytic materials for liquid phase reactions [23-25]. These carbides have a  
86 better stability than sulphides together with similar catalytic properties than noble

87 metals [25, 26]. Among the different metal carbides, Mo<sub>2</sub>C has recently appeared as a  
88 promising material to be used as the catalyst for HDO reactions. Although Mo<sub>2</sub>C might  
89 be less active than noble metals under some reaction conditions, it is indeed more  
90 efficient in terms of O-removal with a minimal hydrogen consumption [23], thus  
91 intensely increasing the hydrogen efficiency of the HDO process. The supports  
92 commonly used for metal carbides include metal oxides (Al<sub>2</sub>O<sub>3</sub>, SiO<sub>2</sub>, ZrO<sub>2</sub>) [18, 27,  
93 28], zeolites (HZSM-5) [18, 23, 29], active carbon [25, 30-33] and bio-char [34].  
94 However, these supports also have the shortcomings described above, and novel  
95 supports need to be tested and developed for the synthesis of active, selective and  
96 resistant Mo<sub>2</sub>C supported catalysts.

97

98 On this matter, carbonaceous materials are considered appropriate catalytic supports for  
99 the synthesis and development of catalysts based on Mo<sub>2</sub>C. In the midst of the different  
100 carbon materials, carbon nanofibres (CNF) are regarded as excellent catalyst supports  
101 for liquid phase reactions due to their high chemical stability in non-oxidising  
102 environments, their tuneable chemical nature and their outstanding textural properties  
103 [33, 35]. In addition, since one of the most common methodologies to synthesise Mo<sub>2</sub>C  
104 is the temperature programmed reaction, in which a molybdenum precursor is heated up  
105 in the presence of a carburising gas [36], CNF themselves can be used as the carbon  
106 source during the carburisation process by simply employing H<sub>2</sub> as the carburising  
107 agent. This strategy dispense with the need of using hydrocarbons in the carburisation  
108 process, thus preventing the counterproductive formation of coke on the Mo<sub>2</sub>C surface  
109 [37]. Despite these outstanding properties, to the best of the authors' knowledge, the  
110 work conducted addressing the use of Mo<sub>2</sub>C/CNF catalysts for the hydrodeoxygenation  
111 (HDO) of lignocellulosic bio-oil is very scarce and all the publications reported to date

112 have used guaiacol (2-methoxyphenol) as a bio-oil model compound. Guaiacol, found  
113 in large quantities in bio-oils produced from lignocellulosic biomass [23, 38, 39], is a  
114 good representative of the phenolic compounds derived from the thermal decomposition  
115 of lignin [40]. Moreover, this chemical owns the most typical functionalities found in  
116 lignin derived phenolic monomers, which allows establishing a reliable comparison  
117 between the removal of oxygen from the hydroxylic (-OH) and methoxy (-OCH<sub>3</sub>)  
118 groups and the hydrogenation of the phenyl group [39, 41-45]. In addition, it must be  
119 borne in mind that it is thermodynamically more difficult to remove oxygen from the  
120 phenolic-derived bio-oil compounds than from those obtained from the biomass  
121 carbohydrate content (cellulose and hemicellulose) [42]. Therefore, the efficiency of the  
122 catalysts will be determined by their capacity to upgrade lignin derived bio-oil  
123 constituents, thus making guaiacol a suitable chemical to test not only the behaviour of  
124 different HDO catalysts, but also the effects of the operating conditions on the process.  
125 Likewise, from a global perspective, it is also more attractive to produce alternative bio-  
126 fuels from the lignin fraction than from the carbohydrate (cellulose and hemicellulose)  
127 biomass fraction due to the lower O/C ratio of the former than the latter [39, 42].

128

129 The publications addressing the use of Mo<sub>2</sub>C/CNF catalysts for the HDO of guaiacol  
130 have largely focused on catalyst development (catalyst synthesis and properties, testing  
131 the catalysts at only some HDO common conditions), rather than on the evaluation of  
132 the influence of all the operating conditions during the HDO process. Ochoa et al. [44]  
133 evaluated the effect of the carburisation temperature (550-750 °C) and heating rate (1-10  
134 °C/min) on the properties and performance of a Mo<sub>2</sub>C/CNF catalyst during the HDO of  
135 guaiacol in a batch reactor operated at 300 °C, 20 bar initial H<sub>2</sub> pressure for 2 h. They  
136 found that high carburisation temperatures and low heating rates improved the catalytic

137 activity of the catalyst under the HDO conditions tested. Moreira et al. [46] used a  
138 Mo<sub>2</sub>C catalyst supported on commercial CNF for the HDO of guaiacol, evaluating the  
139 effect of the temperature (300 and 350 °C), initial H<sub>2</sub> pressure (20 and 30 bar) and  
140 reaction time (2 and 4 h). Increasing the temperature and/or reaction time increased the  
141 guaiacol conversion, but also augmented the proportion of high molecular weight  
142 compounds in the reaction mixture, while augmenting the H<sub>2</sub> pressure led to increases  
143 in the guaiacol conversion and phenol selectivity. Jongerius et al. [47] evaluated the  
144 performance of a Mo<sub>2</sub>C/CNF catalyst during the HDO of guaiacol at different  
145 temperatures (300-350 °C) and reaction times (0-6 h) using a H<sub>2</sub> pressure of 55 bar.  
146 They reported that long reaction times and high temperatures increased the guaiacol  
147 conversion and the production of benzene and toluene. Liu et al. [23] analysed the  
148 effects of the temperature (330-375 °) and reaction time (0-300 min) in a 300 mL batch  
149 reactor using an initial H<sub>2</sub> pressure of 34 bar, achieving a complete guaiacol conversion  
150 in 250 min at 300 °C. Increasing the temperature and reaction time increased the  
151 guaiacol conversion. As a result, a complete conversion was achieved in 120 min at 375  
152 °C. In addition, they reported that the HDO of guaiacol over Mo<sub>2</sub>C/CNF catalysts  
153 occurred by the direct demethoxylation of guaiacol yielding phenol, followed by Ar-OH  
154 bond cleavage to produce benzene at high temperatures, as Mo<sub>2</sub>C is very efficient in  
155 terms of O-removal with minimal H<sub>2</sub> consumption [48].

156

157 These publications provide useful information about the synthesis, characterisation and  
158 performance of several Mo<sub>2</sub>C/CNF catalysts. Nonetheless, since different reactors,  
159 operating conditions and catalyst types were used, the comparison between the different  
160 data available in the literature is unreliable. Therefore, new insights must be gained into  
161 the effects of the operating conditions during the HDO of guaiacol over Mo<sub>2</sub>C/CNF

162 catalysts. Given this scenario, this work firstly evaluates the effects of the temperature  
163 (270-330 °C), reaction time (0-180 min), catalyst loading (0-0.15 g cat/g guaiacol),  
164 initial H<sub>2</sub> pressure (20-60 bar), H<sub>2</sub>/guaiacol ratio (1.5-13.6 mol/mol) and liquid reaction  
165 volume (120-200 mL) on the HDO of guaiacol using a Mo<sub>2</sub>C/CNF catalyst. This  
166 includes the analyses of the effects of these operating conditions on the reaction  
167 pathway, guaiacol conversion, HDO efficiency and chemical composition of the liquid  
168 fraction produced during the experiments. Therefore, the rigorous parametric study  
169 conducted, together with the limited amount of experimental data available in the  
170 literature carefully evaluating the effects of the operating conditions over Mo<sub>2</sub>C/CNF  
171 catalysts, demonstrate that this work represents a novel and challenging investigation in  
172 this field.

173

## 174 **2. Experimental**

### 175 **2.1 Catalyst preparation and characterisation**

176 A Mo<sub>2</sub>C supported on CNF catalyst was used for the experiments. The catalyst  
177 preparation comprises two consecutive steps: the synthesis of the support; i.e. the  
178 carbon nanofibres (CNF), and the subsequent incorporation of Mo<sub>2</sub>C on the fibres. The  
179 CNF were produced by means of a synthetic biogas (CH<sub>4</sub>:CO<sub>2</sub>; 50:50 vol/vol)  
180 decomposition over a Ni:Co:Al (33.5:33.5:33; wt.%) catalyst using a rotatory bed  
181 reactor at 650 °C. Then, the CNF were functionalised in a two-step process: sonicated in  
182 HCl at 60 °C (aimed to remove the possible metal content derived from the catalyst used  
183 in the decomposition reaction) followed by HNO<sub>3</sub> treatment at boiling point in order to  
184 create oxygen groups on their surface, as these groups facilitate the dispersion of the  
185 active phase when the catalyst precursor is deposited onto the fibres. More details about  
186 the CNF synthesis and characterisation can be found elsewhere [44]. The Mo<sub>2</sub>C was

187 incorporated on the CNF by incipient wetness impregnation using a  
188  $(\text{NH}_4)_6\text{Mo}_7\text{O}_{24}\cdot 4\text{H}_2\text{O}$  aqueous solution. The solution was prepared to obtain a catalyst  
189 with a  $\text{MoO}_3$  content of 15 wt.%. After the impregnation, a carbothermal hydrogen  
190 reduction (CHR) was conducted, using a temperature program optimised in a previous  
191 work [44]. Briefly, the CHR was carried out in a fixed-bed tubular quartz reactor (75 cm  
192 in length and 15 mm of internal diameter) using 100 mL STP/min of  $\text{H}_2$  at 750 °C and  
193 atmospheric pressure. This temperature was reached in two steps: a first increase up to  
194 350 °C at a rate of 10°C/min, followed by a second increase up to 750 °C at a rate of 1  
195 °C/min up and a third 1 h isothermal period. Finally, the reactor was cooled down under  
196 a  $\text{N}_2$  atmosphere and the active catalyst was passivated with an  $\text{O}_2/\text{N}_2$  (1/99 vol.%)  
197 mixture using a flow rate of 24 mL STP/min at 25 °C for 2 h.

198

199 The characterisation of the catalyst revealed that the prepared  $\text{Mo}_2\text{C}/\text{CNF}$  catalyst has a  
200 Mo content of 12.9 wt.% (measured by ICP, Inductive Couple Plasma, analysis)  
201 supported on a CNF resembling a fishbone-type structure (observed by Transmission  
202 Electron Microscopy, TEM). The crystallinity of the catalyst determined by XRD (X-  
203 Ray Diffraction) and the crystal size of the Mo phases were calculated by using the  
204 diffractometry suite TOPAS. In these analyses three phases were observed: graphitic  
205 carbon from CNF,  $\text{Mo}_2\text{C}$  peaks related to the hexagonal close packing structure ( $\beta$ -  
206  $\text{Mo}_2\text{C}$ ) of 10.9 nm and small crystals of less than 2 nm of  $\text{MoO}_2$  as a consequence of  
207 CHR process. The XPS (X-ray Photoelectron Spectroscopy) spectra revealed the  
208 coexistence of  $\text{Mo}^{2+}$ , related to  $\text{Mo}_2\text{C}$ , and  $\text{Mo}^{\delta+}$  ( $2+ < \delta+ < 4+$ ), commonly named  
209 molybdenum oxycarbides (Mo-C-O), corresponding to an intermediate state between  
210  $\text{Mo}_2\text{O}$  and  $\beta\text{-Mo}_2\text{C}$ . The catalyst showed a BET (Brunauer–Emmett–Teller) surface area  
211 of 64.2  $\text{m}^2/\text{g}$  and a total pore volume of 0.398  $\text{cm}^3/\text{g}$ . The porous were largely

212 mesoporous (40-70 nm) with a small volume of micropores (1-1.5 nm) according to the  
213 DFT (Discrete Fourier Transform) analysis. More information about the  
214 characterisation of the catalyst can be found elsewhere [44].

215

## 216 **2.2 Experimental reaction system**

217 A 300 mL autoclave batch reactor (Parker Autoclave Engineers) connected to a liquid  
218 sampler was used for the HDO experiments. The reactor is heated up by an external  
219 heating jacket and the reaction temperature is monitored and controlled by means of a  
220 thermocouple connected to a PID control. A stirrer bar, controlled by a magnetic rotor  
221 (Magnedrive), was used to homogenise the reaction mixture, while a coil tube and a  
222 baffle helped to create a turbulent regime in order to facilitate the diffusion of H<sub>2</sub> in the  
223 liquid. To analyse the evolution over time of the HDO reaction, several aliquots were  
224 withdrawn by means of a liquid sampler, containing a solid filter on its tip to prevent  
225 solid loss, connected to the reactor.

226

## 227 **2.3 Experimental procedure, operating conditions and data analysis**

228 The experiments to assess the effect of the operating conditions on the process were  
229 conducted with a 3 vol.% guaiacol/n-decane solution (both chemicals, guaiacol used as  
230 the reactant and n-decane as the solvent, with a purity greater than 99%). The guaiacol  
231 concentration and the solvent were chosen having regard to previous works addressing  
232 the HDO of guaiacol [20, 22, 44, 46, 47]. For the experiments, the reactor was loaded  
233 with 120 or 200 mL of the 3 vol.% guaiacol/n-decane solution and different amounts of  
234 catalyst depending on the process conditions. Then, it was closed and two leak tests, one  
235 with N<sub>2</sub> and other with H<sub>2</sub>, were conducted using a similar pressure to that achieved at  
236 reaction conditions. Afterwards, the reactor was purged with 300 mL STP/min of H<sub>2</sub> for

237 15 min in order to remove all the air and N<sub>2</sub> from the vessel, creating a H<sub>2</sub> atmosphere.  
238 Then, the reactor was pressurised with more H<sub>2</sub> and heated up to the reaction  
239 temperature. In these steps, a stirring rate of 300 rpm was used in order to minimise the  
240 turbulence to prevent any significant reaction. Once the reaction temperature was  
241 achieved, the rotation speed was increased up to 1000 rpm.

242

243 The progress of the reaction was analysed with time by withdrawing different aliquots  
244 during the reaction process, purging the sampling line before collecting each aliquot.  
245 Once the reaction time was complete, the stirring speed was diminished down to 300  
246 rpm and the reactor let cool to room temperature. Then, the pressure was released, the  
247 gas phase analysed and the reaction vessel opened to recover the catalyst and the liquid  
248 reaction mixture. After the HDO experiments, three fractions were obtained. A liquid  
249 fraction, comprising the unreacted guaiacol and the reaction liquid products dissolved in  
250 decane as the solvent; the spent gas phase and a solid fraction consisting of the spent  
251 catalyst. The gas phase was analysed using a micro gas chromatograph (micro GC  
252 Varian CP4900) equipped with two packed columns, molecular sieve and porapak,  
253 coupled to a TCD detector. The liquid product recovered after the experiment was  
254 separated from the spent solid by filtration using a filtration funnel. All the liquid  
255 samples, including the liquid product recovered from the reactor at the end of the  
256 experiment and all the aliquots collected over the course of the reaction were filtered  
257 using a 20 µm filter syringe prior to their analysis. In the sampling step, less than 0.05%  
258 of the catalyst loaded in the reactor was recovered in the filter; thus indicating a  
259 negligible catalyst loss during the sampling process. The solid fraction, consisting of the  
260 spent catalyst, was rinsed with ethanol and dried overnight at 60 °C in an oven. Then the  
261 liquid and solid fractions were stored for further analyses. The mass balance conducted

262 at the end of the experiment confirmed that 99% of the catalyst initially loaded in the  
263 reactor was recovered. All the liquid samples collected, i.e. the aliquots obtained during  
264 the course of the reaction together with the liquid recovered after the experiment, were  
265 analysed in a Gas Chromatographer (CLASUS 5080 Perkim Elmer) coupled with a FID  
266 detector. The identification and quantification of the unreacted guaiacol and liquid  
267 products were performed as described elsewhere [44, 46].

268

269 The parametric analysis comprises the effects of the temperature (270-330 °C), reaction  
270 time (0-180 min), catalyst loading (0-0.15 g cat/g guaiacol), initial H<sub>2</sub> pressure (20-60  
271 bar), H<sub>2</sub>/guaiacol ratio (1.5-13.3 mol/mol) and liquid reaction volume (120-200 mL) on  
272 the process. The effects of the temperature, initial H<sub>2</sub> pressure and reaction time were  
273 evaluated using a total liquid volume of 200 mL. The influences of the H<sub>2</sub>/guaiacol ratio  
274 and total liquid volume were evaluated using two liquid volumes: 120 and 200 mL,  
275 which varied the free volume between 180 and 100 mL (considering the total volume of  
276 the reactor, 300 mL), respectively. This variation in the free volume allows the analyses  
277 of the effects on the process of the H<sub>2</sub>/guaiacol ratio using the same initial H<sub>2</sub> pressure.  
278 Likewise, the same H<sub>2</sub>/guaiacol ratio can be achieved using different liquid volumes and  
279 initial H<sub>2</sub> pressures. These effects were evaluated on the guaiacol conversion, HDO  
280 efficiency and liquid product composition (solvent and un-reacted guaiacol free), which  
281 were calculated according to Eq. 1-3, respectively.

282

$$283 \quad \text{Conversion (\%)} = \frac{\text{initial guaiacol (g)} - \text{final guaiacol (g)}}{\text{initial guaiacol (g)}} \quad (\text{Eq. 1})$$

$$284 \quad \text{Product composition (wt. \%)} = \frac{\text{amount of product (solvent and guaiacol free) (g)}}{\text{total reaction products (solvent and guaiacol free) (g)}} \quad (\text{Eq. 2})$$

$$285 \quad \text{HDO efficiency (\%)} = \frac{\text{oxygen in the feed (g)} - \text{oxygen in the quantified products (guaiacol free) (g)}}{\text{oxygen in the feed (g)}} \quad (\text{Eq. 3})$$

286

287

### 288 **3. Results and discussion**

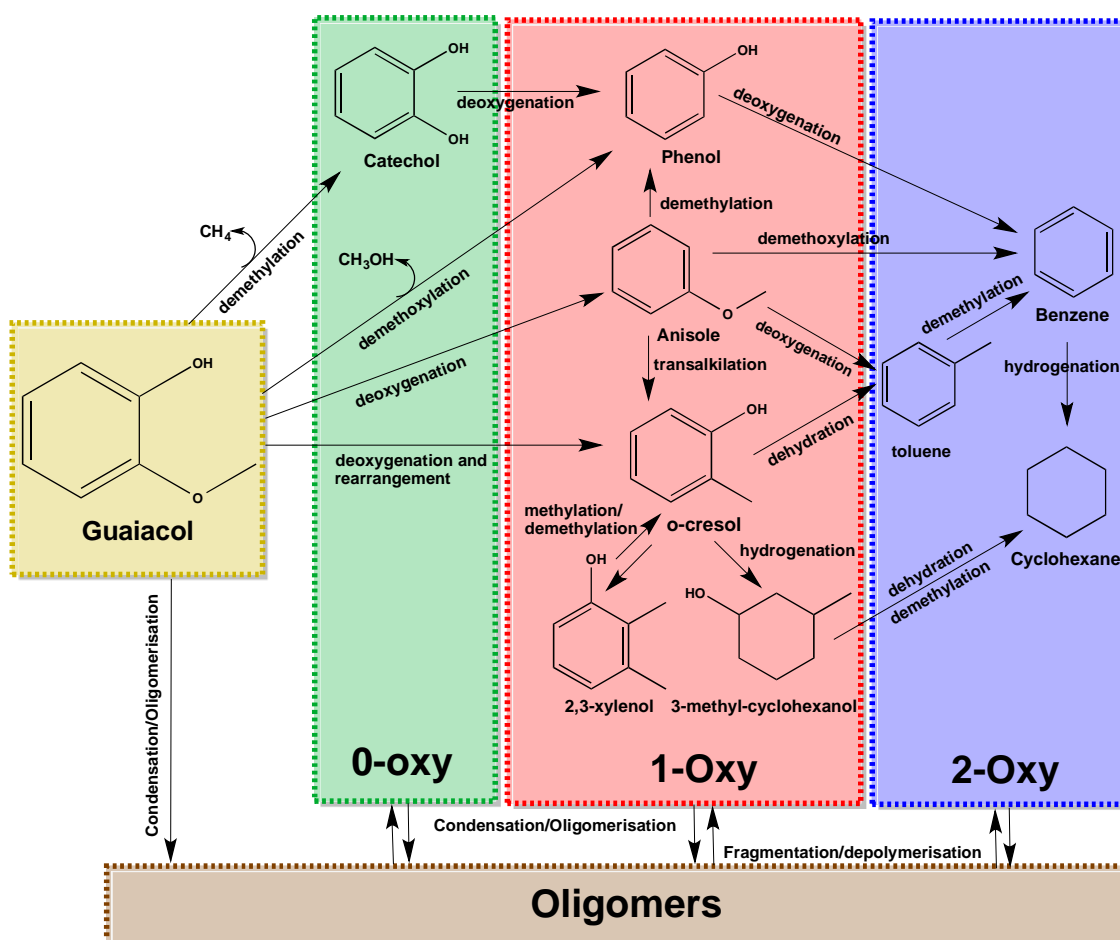
#### 289 **3.1 Possible reaction pathway during the HDO of guaiacol**

290 Three different fractions were recovered after the HDO experiments: gas, solid and  
291 liquid. The gas phase is largely made up of the H<sub>2</sub> initially loaded in the reactor, while  
292 the solid fraction recovered after the experiment consists of the spent Mo<sub>2</sub>C/CNF  
293 catalyst. The liquid phase comprises unreacted guaiacol together with different reaction  
294 products dissolved in decane. Attending to the number of oxygen atoms removed from  
295 the original guaiacol structure, these species can be classified into three categories [23]:  
296 2 oxygen atoms removed (2-oxy), 1 oxygen atom removed (1-oxy) and non-oxygen  
297 removed (0-oxy). 2-oxy compounds include toluene, benzene and cyclohexane; 1-oxy  
298 compounds comprise phenol, anisole, o-cresol, 2,3-xylenol and 3-methyl-ciclohexanol;  
299 while 0-oxy compounds contain catechol. In addition, the mass balance conducted  
300 revealed the formation via condensation reactions of soluble, high molecular weight  
301 species, namely high molecular weight oligomers, which could not be detected by Gas  
302 Chromatography [23, 44, 47].

303

304 Figure 1 shows a possible reaction pathway for the HDO of guaiacol over the  
305 Mo<sub>2</sub>C/CNF catalyst based on the liquid reaction products distribution obtained in the  
306 experiments. The HDO of guaiacol largely comprises demethylation, demethoxylation,  
307 deoxygenation, transalkylation, methylation and dehydrogenation reactions [23, 42, 44-  
308 46, 49, 50]. At early reaction stages, guaiacol can decompose into 0-oxy compounds  
309 (catechol), via a demethylation reaction and 1-oxy compounds through demethoxylation  
310 and deoxygenation reactions. Guaiacol demethoxylation leads to the production of  
311 phenol, while its deoxygenation yields anisole and o-cresol [23, 43-46], this latter via a

312 first deoxygenation reaction followed by subsequent rearrangements [46].  
 313 Subsequently, catechol and anisole can be deoxygenated and demethylated,  
 314 respectively, to produce phenol [43-46]. In addition, o-cresol can also be produced from  
 315 anisole via a transalkylation reaction, while toluene can also be obtained from anisole  
 316 and o-cresol via deoxygenation and dehydration reactions, respectively [41, 44-46]. O-  
 317 cresol can undergo a subsequent methylation reaction to produce 2,3-xyleneol or a  
 318 hydrogenation reaction to give 3-methyl-cyclohexanol. Afterwards, benzene, which can  
 319 be latterly hydrogenated to cyclohexane, can be produced from the deoxygenation of  
 320 phenol and/or demethylation of toluene. In addition, cyclohexane can also be produced  
 321 from 3-methyl-cyclohexanol through a hydration/demethylation reaction [41, 44-46].



322

323 Figure 1. Possible reaction pathway during the hydrodeoxygenation of guaiacol over a  
 324 Mo<sub>2</sub>C/CNF catalyst.

325

326 In addition, condensation, polymerisation and oligomerisation reactions occur during  
327 the HDO of guaiacol, especially in the absence of a catalyst [23, 44, 46, 47]; these  
328 reactions leading to the formation of high molecular weight species, namely oligomers.  
329 These molecules can also undergo cracking, depolymerisation and fragmentation  
330 reactions leading to the formation of low molecular weight species and contributing to  
331 the formation of 0-oxy, 1-oxy and 2-oxy compounds.

332

### 333 **3.2 Effects of the operating conditions during the HDO of guaiacol**

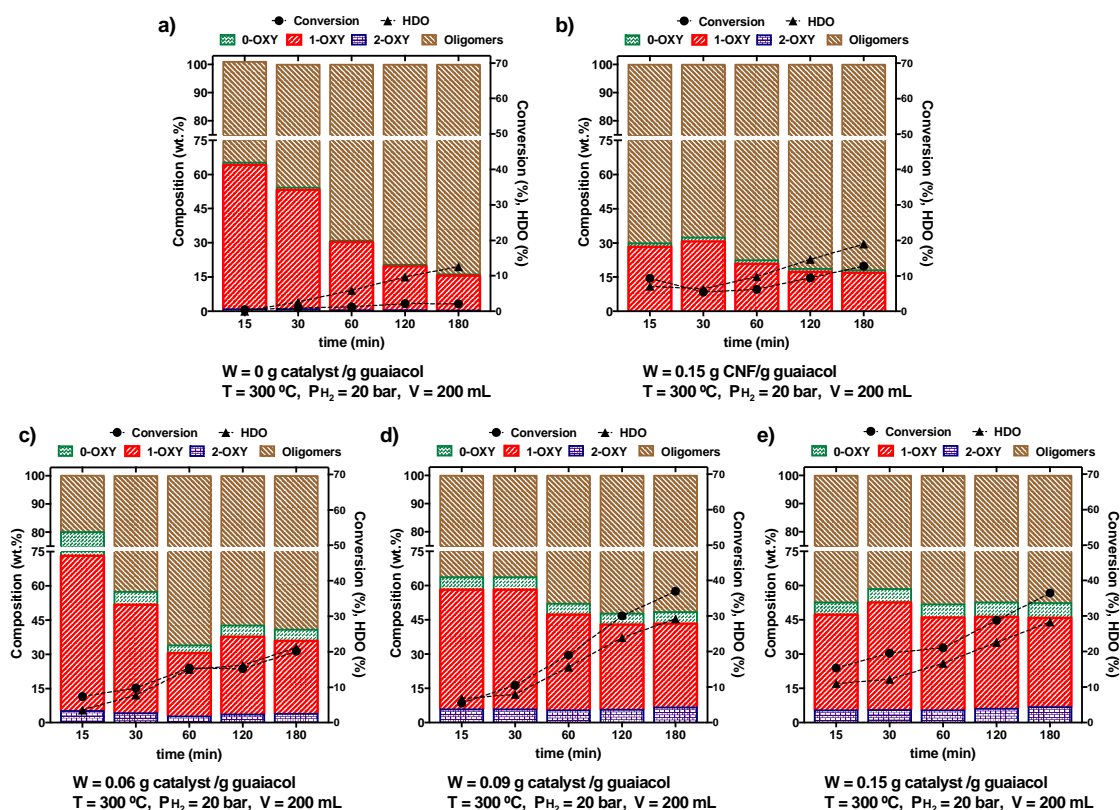
334 Regardless of the operating conditions, gas and solid formation was negligible; the gas  
335 phase largely consisting of the H<sub>2</sub> initially loaded in the reactor (97-99 vol.%), with  
336 small amounts of CO<sub>2</sub> (0-1 vol.%) and CH<sub>4</sub> (0.5-2 vol.%) and the solid fraction  
337 comprising the spent Mo<sub>2</sub>C/CNF catalyst. This indicates a negligible formation of gases  
338 and solid species such as humins, char and/or coke at the operating conditions used in  
339 this work. The liquid phase consists of unreacted guaiacol together with different  
340 reaction products dissolved in decane, whose precise chemical composition strongly  
341 depends on the HDO conditions. Given these results, the effects of the operating  
342 conditions during the HDO of guaiacol have been assessed analysing the guaiacol  
343 conversion (%), liquid product composition (solvent and un-reacted guaiacol free,  
344 wt.%) and HDO efficiency (un-reacted guaiacol and oligomers free) (%). In particular,  
345 the effects of the catalyst loading, initial H<sub>2</sub> pressure, reaction temperature, initial  
346 H<sub>2</sub>/guaiacol ratio and liquid reaction volume are discussed next. The detailed liquid  
347 compositions obtained in the experiments are provided in the supplementary  
348 information.

349

350

### 351 3.2.1 Catalyst loading

352 Figure 2 shows the effects of the catalyst loading on the HDO of guaiacol at 300 °C,  
 353 using an initial H<sub>2</sub> pressure of 20 bar (60 bar at reaction conditions) and a liquid  
 354 reaction mixture of 200 mL. Two non-catalytic experiments were conducted: a pure  
 355 non-catalytic experiment (blank test) without any catalyst and semi-blank test, using  
 356 0.15 g of carbon nanofibres (CNF) to test the possible catalytic activity of the support.  
 357 Figures 2 a and b plot the evolution over time of the guaiacol conversion, HDO  
 358 efficiency and liquid product composition in the absence of a catalyst (0 g catalyst/ g  
 359 guaiacol) and using the prepared CNF (prior to Mo<sub>2</sub>C incorporation) as the catalyst,  
 360 respectively. In addition, Figures 2 c-e show these effects for catalyst/guaiacol ratios of  
 361 0.06, 0.09 and 0.15 g catalyst/guaiacol. Tables S1a-e list the detailed liquid product  
 362 composition.



363

364 Figure 2. Evolution over time of the guaiacol conversion, HDO efficiency and liquid  
 365 product distribution (un-reacted guaiacol and solvent free) using different catalyst  
 366 loadings.

367 In the absence of a catalyst, the guaiacol conversion and HDO efficiency are very low  
368 regardless of the reaction time (0-180 min). The liquid phase is largely made up of 1-  
369 oxy products and high molecular weight soluble oligomers. The large proportion of this  
370 latter species in the liquid product is accounted for by the great spread of condensation,  
371 polymerisation and oligomerisation reactions occurring during the HDO of guaiacol in  
372 the absence of a catalyst [23, 44, 46, 47]. Increasing the reaction time leads to a small  
373 increase in the guaiacol conversion and HDO efficiency together with a substantial  
374 increase in the relative amount of high molecular weight species in the liquid product,  
375 due the progressive extension of condensation and oligomerisation reactions with the  
376 course of the reaction [46, 47, 51].

377

378 Using the CNF as the catalyst for the HDO of guaiacol leads to an increase in the  
379 guaiacol conversion and HDO efficiency in comparison to the results obtained without a  
380 catalyst, which indicates that the fibres on their own (without Mo<sub>2</sub>C) possess some  
381 catalytic activity. These differences are notably marked at early reaction stages, as the  
382 positive catalytic effect of the fibres allows achieving the same degree of conversion  
383 obtained in the absence of a catalyst using a much shorter reaction time. The liquid  
384 product largely comprises high molecular weight oligomers together with small  
385 amounts of 0-oxy and 1-oxy compounds. In addition, the reaction time exerts a  
386 significant influence. While an initial increase in the reaction time between 0 and 60  
387 min does not substantially increase the guaiacol conversion, HDO efficiency or liquid  
388 product distribution, a further increase up to 180 min not only does lead to increases in  
389 the guaiacol conversion and HDO efficiency, but also it modifies the composition of the  
390 liquid product. In particular, the proportion of 1-oxy compounds decreases and the  
391 relative amount of high molecular weight species increases. This is believed to be the

392 consequence of the greater extension of condensation and oligomerisation reactions of  
393 guaiacol occurring in the absence of a selective hydrodeoxygenation catalyst, which  
394 increases the guaiacol conversion but decreases the selectivity towards desired HDO  
395 products [44, 46, 47, 51].

396

397 The catalyst loading has a significant influence on the HDO of guaiacol at the operating  
398 conditions tested in this work. Regardless of the reaction time, an initial increase in the  
399 amount of catalyst from 0 to 0.09 g catalyst/g guaiacol (Figures 2 a, c and d)  
400 significantly increases the guaiacol conversion and HDO efficiency due to the positive  
401 effect of the catalyst on demethylation, demethoxylation, deoxygenation,  
402 transalkylation, methylation and hydrogenation reactions [23, 42, 44-46]. In addition,  
403 this increase in the catalyst amount also modifies the composition of the liquid product.  
404 In particular, the proportion of oligomers decreases at expense of the increase in the  
405 relative amount of HDO products (2-oxy, 1-oxy and 0-oxy compounds) due to the  
406 positive catalytic effect of the catalyst on the process [23, 45, 46]. Increasing the  
407 guaiacol conversion decreases the proportion of oligomers in the liquid product, as  
408 some intermediate 1-oxy products, such as phenol and cresol, are more stable against  
409 self-condensation than guaiacol, thus decreasing the formation of these macromolecular  
410 species [47, 51]. In addition, it might be also possible that the oligomers produced can  
411 be transformed into low molecular weight compounds via fragmentation,  
412 depolymerisation and cracking reactions. Among the HDO products, the relative  
413 amounts of 0-oxy and 2-oxy compounds increase, while the concentration of 1-oxy  
414 compounds remains relatively steady for the first 60 min of reaction and increases  
415 afterwards (60-180 min). At early reaction stages, the proportion of 1-oxy compounds is  
416 not greatly affected by the catalyst loading due to the compensation of two

417 developments: the decrease in the relative amount of oligomers and the increase in the  
418 proportion of 2-oxy species produced from 1-oxy compounds. Conversely, when a  
419 longer reaction time is used (60-180 min), increasing the catalyst amount also leads to  
420 an increase in the guaiacol conversion; however, the amount of catalyst and/or H<sub>2</sub> in the  
421 reactor is not sufficient to transform 1-oxy compounds into 2-oxy compounds; and  
422 consequently, 1-oxy compounds accumulate.

423

424 A further increase in the catalyst amount from 0.09 to 0.15 g catalyst/g guaiacol results  
425 in two different outcomes depending on the reaction time. On the one hand, when a  
426 short reaction time (0-30 min) is used, increasing the catalyst loading leads to small  
427 increases in the guaiacol conversion and HDO efficiency. On the other, between 60 and  
428 180 min, this same increase in the catalyst loading does not exert a significant influence  
429 on the guaiacol conversion or HDO efficiency. In addition, the overall composition of  
430 the liquid phase is not substantially modified with increasing the catalyst loading from  
431 0.09 to 0.15 g catalyst/g guaiacol. Specifically, while at early reaction stages (between 0  
432 and 30 min), moderate increases and decreases take place for the proportions of  
433 oligomers and 1-oxy compounds, respectively, non-significant variations are observed  
434 in the composition of the liquid product between 60 and 180 min. However, this  
435 increase in the catalyst loading does significantly modify the composition of 1-oxy  
436 compounds. In particular, the proportion of phenol decreases, while the relative amount  
437 of 2,3-xyleneol increases, thus suggesting the progressive transformation of the former in  
438 the latter due to the greater amount of catalyst in the reactor (Table S1e).

439

440 These developments are believed to be a consequence of a possible H<sub>2</sub> limitation; i.e. a  
441 limited amount of H<sub>2</sub> dissolved in the reaction medium (decane) under some conditions.

442 Under the operating conditions tested (200 mL of a 3 vol.% guaiacol solution, 300 °C,  
443 60 bar of H<sub>2</sub> and a liquid reaction mixture of 200 mL), the maximum H<sub>2</sub>/guaiacol ratio  
444 that could be achieved in the experiment (if all the H<sub>2</sub> initially loaded in the reactor was  
445 effectively dissolved in the decane solution) is 1.51 mol H<sub>2</sub>/mol guaiacol. Taking into  
446 account the thermodynamic solubility of H<sub>2</sub> in decane at reaction conditions (0.63 mol  
447 H<sub>2</sub>/kg decane [52]), the maximum thermodynamic H<sub>2</sub>/guaiacol ratio that can be  
448 achieved is 2.61 mol H<sub>2</sub>/mol guaiacol, which is higher than the experimental  
449 H<sub>2</sub>/guaiacol ratio loaded in the reactor. Therefore, the activity of the catalyst might be  
450 limited by the H<sub>2</sub> availability in the reaction medium, this phenomenon also being  
451 controlled by the diffusion of H<sub>2</sub> from the gas to the liquid. Thus, this limited amount of  
452 H<sub>2</sub> in comparison to the amount of guaiacol in the liquid hinders the transformation of  
453 1-oxy into 2-oxy compounds. However, despite this H<sub>2</sub> limitation, a greater amount of  
454 catalyst in the reactor might promote other reactions, such as transalkylation and  
455 methylation, which modifies the reaction pathway. This prevents phenol deoxygenation  
456 due to the limited amount of H<sub>2</sub> in the reaction medium, favouring its transformation  
457 into 2,3-xyleneol instead, via a first transalkylation to o-cresol followed by a  
458 methylation reaction. As a result, non-significant variations are observed for the total  
459 proportions of 1-oxy and 2-oxy compounds with increasing the catalyst loading,  
460 especially from 0.09 to 0.15 g catalyst/g guaiacol at long reaction times.

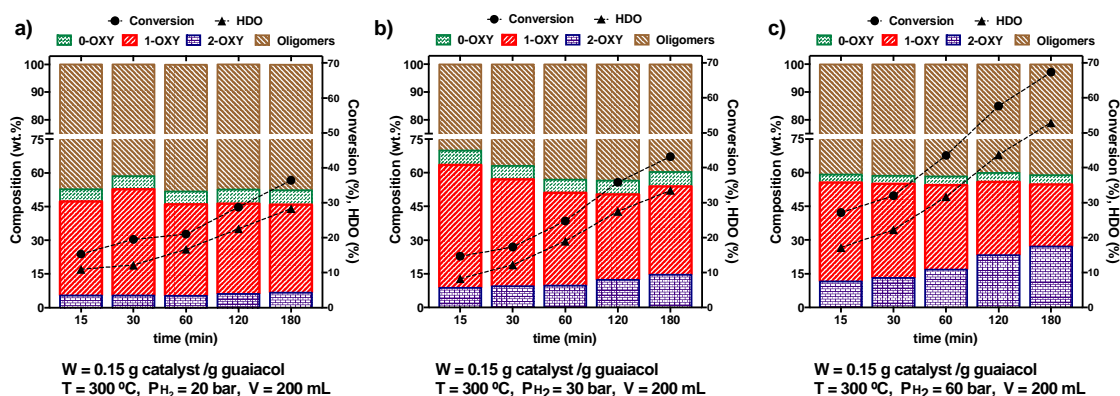
461

### 462 **3.2.2 Initial H<sub>2</sub> pressure**

463 Figure 3 shows the effects of the initial H<sub>2</sub> pressure on the HDO of guaiacol at 300 °C  
464 using a catalyst loading of 0.15 g catalyst/g guaiacol and a liquid reaction volume of  
465 200 mL. In particular, Figures 3 a, b and c plot the evolution over time of the guaiacol  
466 conversion, HDO efficiency and liquid product composition using an initial H<sub>2</sub> pressure

467 of 20, 30 and 60 bar (60, 80 and 120 bar at reaction conditions). Tables S2a-c list the  
468 detailed liquid product composition.

469



471

472 Figure 3. Evolution over time of the guaiacol conversion, HDO efficiency and liquid  
473 product distribution (un-reacted guaiacol and solvent free) using different initial  $H_2$   
474 pressures.

475

476 Figure 3 shows the significant effect of the  $H_2$  pressure on the HDO of guaiacol. An  
477 increase in the initial  $H_2$  pressure from 20 to 60 bar increases the guaiacol conversion  
478 and HDO efficiency and modifies the liquid product distribution. In particular, this  
479 increase in the  $H_2$  pressure leads to an increase in the proportion of HDO products  
480 together with a decrease in the relative amount of high molecular weight oligomers.

481 This is believed to be the result of the greater spread of HDO reactions in comparison to  
482 condensation reactions due to the greater amount of  $H_2$  dissolved in the reaction  
483 medium [23, 45, 46]. Increasing the  $H_2$  pressure not only does upsurge the initial

484  $H_2$ /guaiacol ratio (1.51, 2.28 and 4.55 mol  $H_2$ /mol guaiacol at 20, 30 and 60 bar initial  
485  $H_2$  pressure, respectively) but also it increases the thermodynamic  $H_2$ /guaiacol ratio

486 (2.61, 3.43 and 5.10 mol  $H_2$ /mol guaiacol at 60, 80 and 120 bar of  $H_2$  at reaction  
487 conditions, respectively). This increase in the initial  $H_2$  pressure upsurges both the

488 initial and thermodynamic  $H_2$ /guaiacol ratios, decreasing the difference between them.

This improves the solubility of  $H_2$  in the reaction medium, which might allow reaching

489 experimental H<sub>2</sub>/guaiacol ratios much closer to the thermodynamic values. Therefore,  
490 augmenting the H<sub>2</sub> pressure increases the proportion of 2-oxy compounds, leading to  
491 reductions in the relative amounts of 0-oxy and 1-oxy compounds. This promotes the  
492 progressive conversion of 0-oxy compounds into 1-oxy compounds; this latter species  
493 being subsequently transformed into 2-oxy compounds [23, 45-47]. These variations are  
494 notably more marked when the initial H<sub>2</sub> pressure increases from 30 to 60 bar due to the  
495 greater increase achieved in the H<sub>2</sub>/guaiacol ratio as described above.

496

497 Regardless of the initial H<sub>2</sub> pressure, both the guaiacol conversion and HDO efficiency  
498 increase over time due to the positive effect of the reaction time on the process, leading  
499 to a progressive guaiacol decomposition into less oxygenated products, thus increasing  
500 the conversion and HDO efficiency over time. However, these increases depend on the  
501 initial H<sub>2</sub> pressure; the higher the initial H<sub>2</sub> pressure, the sharper are the increases  
502 observed for the guaiacol conversion and HDO efficiency. In addition, the evolution  
503 over time for the liquid product distribution also depends on the initial H<sub>2</sub> pressure with  
504 different variations taking place. On the one hand, when a low initial H<sub>2</sub> pressure is  
505 used, the liquid composition remains relatively steady over the 3 h reaction. Only minor  
506 decreases and increases over time are observed for the relative amounts of 1-oxy and 2-  
507 oxy compounds, respectively; these variations leading to a soft increase in the HDO  
508 efficiency. On the other hand, increasing the initial H<sub>2</sub> pressure boosts the effect of the  
509 reaction time on the liquid product composition. In particular, sharper increases and  
510 decreases over time are observed with increasing the H<sub>2</sub> pressure for the proportions of  
511 2-oxy and 1-oxy compounds, respectively. The different evolution of these variables  
512 over time might be accounted for by the variations in the experimental H<sub>2</sub>/guaiacol ratio  
513 of the solutions. For a low initial H<sub>2</sub> pressure, the experimental H<sub>2</sub>/guaiacol ratio is quite

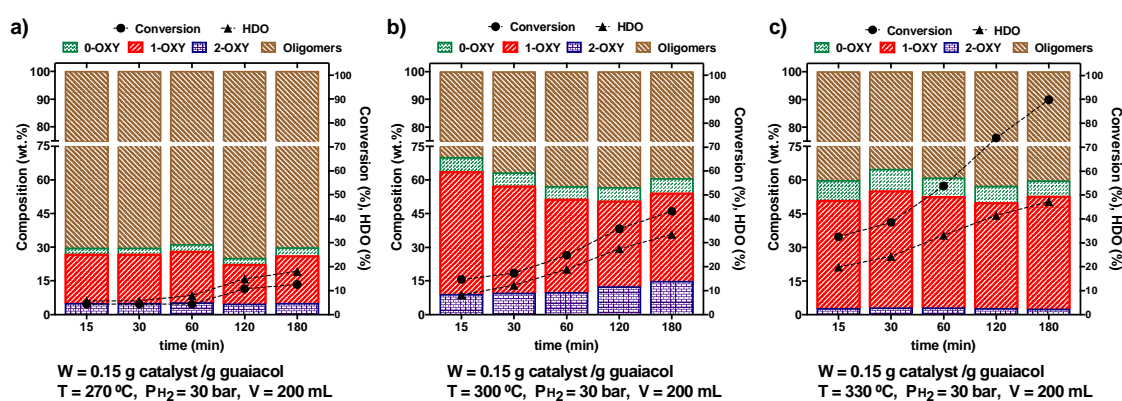
514 low and decreases over the course of the reaction due to the progressive H<sub>2</sub>  
 515 consumption, thus impeding the progress of the reaction and hampering the conversion  
 516 of 1-oxy compounds into 2-oxy species. Conversely, increasing the H<sub>2</sub> pressure  
 517 augments both the initial maximum H<sub>2</sub>/guaiacol ratio and the thermodynamic  
 518 H<sub>2</sub>/guaiacol ratio dissolved in decane at reaction conditions; thus the process is less  
 519 affected by the experimental decrease in the H<sub>2</sub>/guaiacol ratio over the course of the  
 520 reaction.

521

### 522 3.2.3 Reaction temperature

523 Figure 4 shows the effects of the reaction temperature on the HDO of guaiacol using a  
 524 catalyst loading of 0.15 g catalyst/g guaiacol, an initial H<sub>2</sub> pressure of 30 bar and a  
 525 liquid reaction volume of 200 mL. In particular, Figures 4 a, b and c plot the evolution  
 526 over time of the guaiacol conversion, HDO efficiency and liquid product composition  
 527 using a reaction temperature of 270, 300 and 330 °C, respectively. Tables S3a-c list the  
 528 detailed liquid product composition.

529



530

531 Figure 4. Evolution over time of the reaction temperature on the guaiacol conversion,  
 532 HDO efficiency and liquid product distribution (un-reacted guaiacol and solvent free)  
 533 using different reaction temperatures.

534

535 The temperature exerts a significant influence on the guaiacol conversion, HDO  
536 efficiency, liquid product distribution and the evolution of these variables over time.  
537 When a low temperature (270 °C) is used, the guaiacol conversion and the HDO  
538 efficiency are very low, especially during the first 60 min of reaction. In addition, the  
539 liquid product largely comprises high molecular weight oligomers; the proportion of  
540 HDO products in the reaction mixture being lower than 30 wt.% regardless of the  
541 reaction time. An increase in the reaction temperature from 270 to 300 °C substantially  
542 increases the guaiacol conversion and HDO efficiency. In addition, this increase in  
543 temperature leads to a significant decrease in the relative amount of oligomers together  
544 with an increase in the concentration of HDO products. This also results in a greater  
545 amount of 0-oxy, 1-oxy and 2-oxy compounds in the liquid product. A subsequent  
546 increase from 300 to 330 °C leads to a sharp increase in the guaiacol conversion,  
547 augmenting the HDO efficiency very slightly. Although these variations take place  
548 without substantially modifying the proportions of oligomers in the liquid reaction  
549 product, some variations in the distribution of HDO products occur. In particular,  
550 augmenting the temperature from 300 to 330 °C leads to increases in the relative  
551 amounts of 0-oxy and 1-oxy species along with a decrease in the proportions of 2-oxy  
552 compounds; thus explaining the small increase observed in the HDO efficiency.

553

554 It is believed that thermodynamic and kinetic phenomena account for these variations.  
555 At low temperature (270 °C) the catalysts might not be active enough and as a result,  
556 low conversions and HDO efficiencies are observed. In these cases, the liquid product is  
557 largely made up of high molecular weight oligomers resulted from the non-catalytic  
558 decomposition of guaiacol. An initial increase in the temperature from 270 to 300 °C  
559 increases the guaiacol conversion, HDO efficiency and the presence of HDO species in

560 the liquid product mixture due to the positive kinetic effect of the temperature on the  
561 process, thus increasing the activity of the catalyst as well as the reaction rate of the  
562 HDO reactions [47]. A further increase in the temperature also leads to a significant  
563 increase in the guaiacol conversion due to the positive effect of the temperature on some  
564 reactions. However, the composition of the liquid product is controlled  
565 thermodynamically. In particular, deoxygenation and dehydration reactions are  
566 exothermic [53], and therefore, increasing the temperature prevents the development of  
567 these reactions, thus hampering the initial transformation of 0-oxy compounds into 1-  
568 oxy species as well as the subsequent conversion of these latter compounds into 2-oxy  
569 products. In addition, it must be borne in mind that H<sub>2</sub> adsorption on the catalyst surface  
570 is also an exothermic process and an increase in the reaction temperature changes the H<sub>2</sub>  
571 sorption equilibrium [54]. Thus, the decreases in H<sub>2</sub> adsorption and surface coverage  
572 with the increase in the temperature hinder hydrogenation reactions [54].

573

574 As a result of these developments, the proportions of 0-oxy and 1-oxy compounds in the  
575 liquid product increase as the expense of the reduction in the relative amount of 2-oxy  
576 compounds. These variations are clearly observed analysing the detailed liquid product  
577 compositions (Tables S3b and c), as increasing the temperature from 300 to 330 °C  
578 substantially increases the proportion of phenol and decreases the relative amount of  
579 2,3-xyleneol. Furthermore, the initial H<sub>2</sub>/guaiacol ratio is 2.28 mol H<sub>2</sub>/mol guaiacol  
580 regardless of the reaction temperature, while the thermodynamic value depends on the  
581 temperature and pressure achieved in the experiment; i.e. 2.61, 3.43 and 3.51 mol  
582 H<sub>2</sub>/mol guaiacol for the experiments conducted at 270, 300 and 330 °C, respectively.  
583 Therefore, the small variations occurring in the H<sub>2</sub>/guaiacol ratio when the temperature

584 of the experiment increases from 300 to 330 °C supports the thermodynamic limitation  
585 hypothesis.

586

587 With regard to the evolution over time of these variables, Figure 4 shows how such  
588 variations depend on the reaction temperature. At 270 °C, small variations over time are  
589 observed for the guaiacol conversion and HDO efficiency due to the low guaiacol  
590 catalytic conversion achieved at low temperature [47]. In addition, the composition of  
591 the liquid product does not depend on the reaction time, and largely the same product  
592 composition is observed within the 180 min of reaction. Conversely, increasing the  
593 temperature modifies the effect of the reaction time on the process. At medium  
594 temperature (300 °C), sharp increases in the guaiacol conversion and HDO efficiency  
595 take place with the course of the reaction. In addition, the composition of the liquid  
596 product also depends on the reaction time. In particular, even though the relative  
597 amount of high molecular oligomers does not depend on the reaction time, and the same  
598 proportion for these species is observed in the reaction mixture, several variations in the  
599 relative amount of HDO products take place.

600

601 In particular, the proportion of 1-oxy compounds decreases and the relative amount of  
602 2-oxy compounds increases due to the progressive transformation of the former into the  
603 latter compounds over the course of the reaction. This transformation is the  
604 consequence of the positive kinetic effect of the reaction time on the process. In  
605 addition, two counteracting effects might account for the steady value observed in the  
606 relative amount of oligomers. On the one hand, an increase in the reaction time  
607 promotes the formation of oligomers via condensation and radical-induced  
608 rearrangement reactions, thus increasing the proportions of oligomers over time. On the

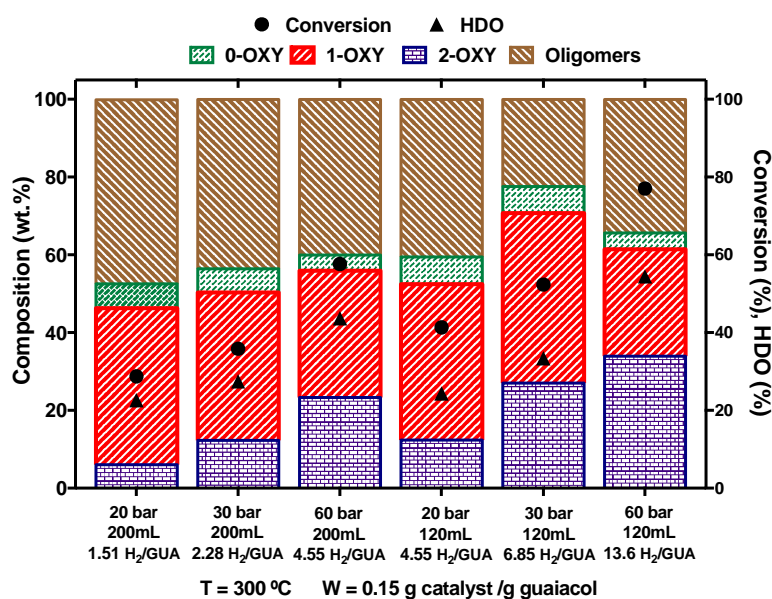
609 other, increasing the reaction time also reduces the amount of guaiacol available to  
610 undergo condensation and radical-induced rearrangement reactions due to the formation  
611 of 1-oxy and 2-oxy species, which are less reactive towards these reactions. In addition,  
612 oligomers can also be transformed into low molecular weight compounds via  
613 depolymerisation, fragmentation and cracking reactions. As a result of this  
614 compensatory effect, the proportion of oligomers remains steady over time. A further  
615 increase in the temperature from 300 to 330 °C modifies the effect of the reaction time  
616 on the process. While the guaiacol conversion displays a substantial increase over time,  
617 the HDO efficiency does not evolve accordingly, and a soft increase is observed for this  
618 variable. In addition, the liquid product distribution is not greatly influenced by the  
619 reaction time. This is the result of the thermodynamic inhibitory effect of the pressure  
620 hindering the transformation of 1-oxy compounds into 2-oxy species [53, 54].  
621 Therefore, although the guaiacol conversion and the production of oligomers and 1-oxy  
622 compounds increase over time, their relative amount in the product mixture remains  
623 constant.

624

#### 625 **3.2.4 Initial H<sub>2</sub>/guaiacol ratio and liquid reaction volume**

626 Figure 5 shows the effects of the H<sub>2</sub>/guaiacol ratio and the liquid reaction volume on the  
627 HDO of guaiacol using a catalyst loading of 0.15 g catalyst/g guaiacol at 300 °C for 120  
628 min. Figure 5 shows the effects of the initial H<sub>2</sub> pressure (20, 30 and 60 bar) using two  
629 reaction liquid volumes: 200 and 120 mL, which allowed varying the initial H<sub>2</sub>/guaiacol  
630 ratio from 1.51 to 4.55 mol H<sub>2</sub>/mol guaiacol and from 4.55 to 13.60 mol H<sub>2</sub>/mol  
631 guaiacol using the large and the small liquid reaction volume, respectively. The H<sub>2</sub>  
632 pressure achieved at reaction conditions (300 °C) using an initial H<sub>2</sub> pressure of 20, 30  
633 and 60 bar is as follows: 60, 80 and 120 bar, using a reaction liquid volume of 200 mL

634 and 34, 50 and 80 bar using a liquid volume of 120 mL. Table S4 lists the detailed  
 635 liquid product composition.



636

637 Figure 5. Effect of the H<sub>2</sub>/guaiacol ratio and liquid reaction volume on the guaiacol  
 638 conversion, HDO efficiency and liquid product distribution (un-reacted guaiacol and  
 639 solvent free).

640

641 The effect of the H<sub>2</sub> pressure on the HDO of guaiacol depends on the liquid reaction  
 642 volume and vice versa. Regardless of the liquid volume, an increase in the initial H<sub>2</sub>  
 643 pressure from 20 to 60 bar leads to an increase in the guaiacol conversion and HDO  
 644 efficiency. However, these increases depend on the reaction volume, with more  
 645 pronounced variations occurring for a small (120 mL) than for a large (200 mL) liquid  
 646 volume. These differences are accounted for by the greater variation occurring in the  
 647 H<sub>2</sub>/guaiacol ratio for the small (120 mL) than for the large (200 mL) liquid volume. A  
 648 300 mL reactor was used in both cases, thus allowing a greater amount of H<sub>2</sub> to be  
 649 loaded in the reactor when using 120 mL than 200 mL at the same initial H<sub>2</sub> pressure.

650

651 In addition, the composition of the liquid phase is also influenced by the initial  
 652 H<sub>2</sub>/guaiacol ratio and liquid reaction volume. When a large reaction volume is used

653 (200 mL), increasing the H<sub>2</sub> pressure leads to an increase in the relative amount of 2-  
654 oxy compounds together with decreases in the proportions of oligomers, 0-oxy and 1-  
655 oxy compounds. This increase in the initial H<sub>2</sub> pressure increases the H<sub>2</sub>/guaiacol ratio,  
656 thus favouring HDO reactions over oligomerisation and condensation reactions [23, 45,  
657 46]. This leads to a decrease in the relative amount of oligomers together with an  
658 increase in the proportions of HDO products in the liquid [46, 47]. Among these, the  
659 proportions of 0-oxy and 1-oxy compounds decrease, while the relative amount of 2-  
660 oxy species increases due to the progressive transformation of 0-oxy and 1-oxy  
661 compounds into fully deoxygenated products [23, 45-47]. Conversely, for a small liquid  
662 reaction volume (120 mL), an initial increase in the initial H<sub>2</sub> pressure from 20 to 30 bar  
663 results in a similar liquid product evolution; i.e. a decrease in the proportions of  
664 oligomers together with an increase in the relative amount of 2-oxy compounds with  
665 minimal variations in the proportions of 0-oxy and 1-oxy compounds. While a further  
666 increase from 30 to 60 bar also increases the relative amount of 2-oxy compounds, the  
667 proportion of oligomers and 1-oxy compounds increases and decreases, respectively.  
668 This suggests the transformation of 1-oxy and 2-oxy compounds into high molecular  
669 weight oligomers via polymerisation and oligomerisation reactions at high guaiacol  
670 conversion levels. As a result, the relative amount of 1-oxy compounds decreases and  
671 the increase in the proportion of 2-oxy compounds is not as pronounced as it could have  
672 been expected attending the increase observed in the guaiacol conversion.

673

674 The comparison between the experiments conducted with the same experimental  
675 H<sub>2</sub>/guaiacol ratio (4.45 mol/mol) using a H<sub>2</sub> pressure and a reaction volume of 60 bar and  
676 200 mL, and 30 bar and 120 mL reveals the relationship between the H<sub>2</sub> pressure and  
677 liquid volume during the HDO of guaiacol. Despite the fact that the same experimental

678 H<sub>2</sub>/guaiacol ratio is used, different results are observed. In particular, a higher guaiacol  
679 conversion and HDO efficiency take place at 60 bar than at 20 bar. In addition, the  
680 liquid product has a higher amount of 2-oxy compounds together with a lower  
681 proportion of 1-oxy species when a high H<sub>2</sub> pressure is used. These differences are  
682 accounted for by the higher thermodynamic H<sub>2</sub>/guaiacol ratio achieved at 60 bar and  
683 200 mL of liquid (5.1 mol H<sub>2</sub>/mol guaiacol) than at 30 bar and 120 mL of liquid (1.25  
684 mol H<sub>2</sub>/mol guaiacol) [52]; thus increasing the H<sub>2</sub> availability in the reaction medium.  
685 This higher amount of H<sub>2</sub> increases the guaiacol conversion and shifts the liquid product  
686 distribution towards the formation of more deoxygenated species (2-oxy compounds),  
687 augmenting the HDO efficiency of the process [23, 45-47].

688

#### 689 **4. Conclusions**

690 This work firstly addresses the effects of the catalyst loading (0-0.15 g cat/g guaiacol),  
691 initial H<sub>2</sub> pressure (20-60 bar), temperature (270-330 °C), reaction time (0-180 min),  
692 H<sub>2</sub>/guaiacol ratio (1.5-13.6 mol/mol) and liquid reaction volume (120-200 mL) on the  
693 hydrodeoxygenation (HDO) of guaiacol, a common lignocellulosic bio-oil representative  
694 molecule, using a Mo<sub>2</sub>C/CNF catalyst. The most important conclusions are summarised  
695 as follows.

696 1. The Mo<sub>2</sub>C/CNF catalyst displayed a positive effect on the HDO of guaiacol. Very  
697 low guaiacol conversions and HDO efficiencies were obtained in the absence of a  
698 catalyst. Conversely, increases over time were observed for the guaiacol conversion and  
699 HDO efficiency in the presence of the Mo<sub>2</sub>C/CNF catalyst. Furthermore, an increase in  
700 the catalyst loading increased the guaiacol conversion and HDO efficiency as well as  
701 the proportions of HDO products in the liquid phase.

702 2. Augmenting the initial H<sub>2</sub> pressure rose the experimental and thermodynamic  
703 H<sub>2</sub>/guaiacol ratios, thus augmenting the H<sub>2</sub> availability in the reaction medium and  
704 therefore, increasing the guaiacol conversion and HDO efficiency. Regardless of the H<sub>2</sub>  
705 pressure, the guaiacol conversion and HDO efficiency increased over time; these  
706 variations being notably marked at elevated H<sub>2</sub> pressure, which promoted the  
707 transformation over time of 1-oxy compounds into fully deoxygenated products.

708 3. The temperature exerted a kinetic promoting effect together with a thermodynamic  
709 inhibitory influence. An initial increase in the temperature increased the guaiacol  
710 conversion, HDO efficiency as well as the proportion of HDO products in the liquid.  
711 Conversely, a subsequent temperature increase hindered the conversion of partially  
712 deoxygenated species into fully deoxygenated products due to the exothermic nature of  
713 some of the chemical reactions involved in such transformations.

714 4. The increases observed in the guaiacol conversion and HDO efficiency as well as the  
715 presence of less oxygenated compounds in the liquid product with increasing the H<sub>2</sub>  
716 pressure depended on the reaction volume, with more pronounced variations occurring  
717 for a small than for a large liquid volume; these differences being the consequence of  
718 the greater variation occurring in the H<sub>2</sub>/guaiacol ratio for former than the latter volume.  
719 In addition, when the same experimental H<sub>2</sub>/guaiacol ratio was attained with two  
720 different initial H<sub>2</sub> pressures and reaction volumes, higher guaiacol conversions, HDO  
721 efficiencies and proportions of fully deoxygenated products were achieved using the  
722 higher initial H<sub>2</sub> pressure and larger volume due to the greater thermodynamic  
723 H<sub>2</sub>/guaiacol ratio achieved.

724

725

726

727 **Acknowledgements**

728 This work was funded by FEDER and the Spanish Economy and Competitiveness  
729 Ministry (MINECO) (ENE2014-52189-C02-01-R and ENE2017-83854-R). Elba Ochoa  
730 thanks for the award of her PhD under the frame of the aforementioned project. In  
731 addition, Javier Remón Núñez would like to express his gratitude to the Spanish  
732 Ministry “Ministerio de Ciencia, Innovación y Universidades” for the Juan de la Cierva  
733 fellowship (FJCI-2016-30847) awarded.

734

735 **References**

- 736 [1] J. Solé, A. García-Olivares, A. Turiel, J. Ballabrera-Poy, Renewable transitions and  
737 the net energy from oil liquids: A scenarios study, *Renewable Energy*, 116 (2018) 258-  
738 271.
- 739 [2] Z. Jiang, P. Zhao, C. Hu, Controlling the cleavage of the inter- and intra-molecular  
740 linkages in lignocellulosic biomass for further biorefining: A review, *Bioresource*  
741 *technology*, 256 (2018) 466-477.
- 742 [3] S. Czernik, A.V. Bridgwater, Overview of Applications of Biomass Fast Pyrolysis  
743 Oil, *Energy & Fuels*, 18 (2004) 590-598.
- 744 [4] M.C. Barnés, M.M. de Visser, G. van Rossum, S.R.A. Kersten, J.P. Lange,  
745 Liquefaction of wood and its model components, *Journal of Analytical and Applied*  
746 *Pyrolysis*, 125 (2017) 136-143.
- 747 [5] J.A. Onwudili, Influence of reaction conditions on the composition of liquid  
748 products from two-stage catalytic hydrothermal processing of lignin, *Bioresource*  
749 *technology*, 187 (2015) 60-69.
- 750 [6] C.E. Efika, J.A. Onwudili, P.T. Williams, Influence of heating rates on the products  
751 of high-temperature pyrolysis of waste wood pellets and biomass model compounds,  
752 *Waste management*, 76 (2018) 497-506.
- 753 [7] M. García-Perez, A. Chaala, H. Pakdel, D. Kretschmer, C. Roy, Characterization of  
754 bio-oils in chemical families, *Biomass and Bioenergy*, 31 (2007) 222-242.
- 755 [8] J. Remón, P. Arcelus-Arrillaga, L. García, J. Arauzo, Production of gaseous and  
756 liquid bio-fuels from the upgrading of lignocellulosic bio-oil in sub- and supercritical  
757 water: Effect of operating conditions on the process, *Energy Conversion and*  
758 *Management*, 119 (2016) 14-36.
- 759 [9] P. Han, G. Nie, J. Xie, X.-t.-f. E, L. Pan, X. Zhang, J.-J. Zou, Synthesis of high-  
760 density biofuel with excellent low-temperature properties from lignocellulose-derived  
761 feedstock, *Fuel Processing Technology*, 163 (2017) 45-50.
- 762 [10] A.V. Bridgwater, Review of fast pyrolysis of biomass and product upgrading,  
763 *Biomass and Bioenergy*, 38 (2012) 68-94.
- 764 [11] S. Ayalur Chattanathan, S. Adhikari, N. Abdoulmoumine, A review on current  
765 status of hydrogen production from bio-oil, *Renewable and Sustainable Energy*  
766 *Reviews*, 16 (2012) 2366-2372.
- 767 [12] K. Jacobson, K.C. Maheria, A. Kumar Dalai, Bio-oil valorization: A review,  
768 *Renewable and Sustainable Energy Reviews*, 23 (2013) 91-106.

- 769 [13] S. Xiu, A. Shahbazi, Bio-oil production and upgrading research: A review,  
770 Renewable and Sustainable Energy Reviews, 16 (2012) 4406-4414.
- 771 [14] Q. Lu, W.-Z. Li, X.-F. Zhu, Overview of fuel properties of biomass fast pyrolysis  
772 oils, Energy Conversion and Management, 50 (2009) 1376-1383.
- 773 [15] J.A. Onwudili, P.T. Williams, Catalytic conversion of bio-oil in supercritical water:  
774 Influence of RuO<sub>2</sub>/γ-Al<sub>2</sub>O<sub>3</sub> catalysts on gasification efficiencies and bio-methane  
775 production, Applied Catalysis B: Environmental, 180 (2016) 559-568.
- 776 [16] L. Cao, I.K.M. Yu, Y. Liu, X. Ruan, D.C.W. Tsang, A.J. Hunt, Y.S. Ok, H. Song,  
777 S. Zhang, Lignin valorization for the production of renewable chemicals: State-of-the-  
778 art review and future prospects, Bioresource technology, 269 (2018) 465-475.
- 779 [17] D. Mohan, C.U. Pittman, P.H. Steele, Pyrolysis of Wood/Biomass for Bio-oil: A  
780 Critical Review, Energy & Fuels, 20 (2006) 848-889.
- 781 [18] Z. He, X. Wang, Hydrodeoxygenation of model compounds and catalytic systems  
782 for pyrolysis bio-oils upgrading, in: Catalysis for Sustainable Energy, 2012, pp. 28.
- 783 [19] M. Fryzuk, Heterogeneous Catalysis in Organic Chemistry By Gerard V. Smith  
784 (Southern Illinois University) and Ferenc Notheisz (József Attila University, Szeged,  
785 Hungary). Academic Press: San Diego, CA. 1999. xvi + 346 pp. \$89.95. ISBN 0-12-  
786 651645-6, Journal of the American Chemical Society, 122 (2000) 5233-5234.
- 787 [20] E.A. Roldugina, E.R. Naranov, A.L. Maximov, E.A. Karakhanov,  
788 Hydrodeoxygenation of guaiacol as a model compound of bio-oil in methanol over  
789 mesoporous noble metal catalysts, Applied Catalysis A: General, 553 (2018) 24-35.
- 790 [21] L. Fan, Y. Zhang, S. Liu, N. Zhou, P. Chen, Y. Cheng, M. Addy, Q. Lu, M.M.  
791 Omar, Y. Liu, Y. Wang, L. Dai, E. Anderson, P. Peng, H. Lei, R. Ruan, Bio-oil from  
792 fast pyrolysis of lignin: Effects of process and upgrading parameters, Bioresource  
793 technology, 241 (2017) 1118-1126.
- 794 [22] A. Gutierrez, R.K. Kaila, M.L. Honkela, R. Slioor, A.O.I. Krause,  
795 Hydrodeoxygenation of guaiacol on noble metal catalysts, Catalysis Today, 147 (2009)  
796 239-246.
- 797 [23] S. Liu, H. Wang, K.J. Smith, C.S. Kim, Hydrodeoxygenation of 2-Methoxyphenol  
798 over Ru, Pd, and Mo<sub>2</sub>C Catalysts Supported on Carbon, Energy & Fuels, 31 (2017)  
799 6378-6388.
- 800 [24] S. Ramanathan, S.T. Oyama, New Catalysts for Hydroprocessing: Transition Metal  
801 Carbides and Nitrides, The Journal of Physical Chemistry, 99 (1995) 16365-16372.
- 802 [25] J. Han, J. Duan, P. Chen, H. Lou, X. Zheng, H. Hong, Nanostructured  
803 molybdenum carbides supported on carbon nanotubes as efficient catalysts for one-step  
804 hydrodeoxygenation and isomerization of vegetable oils, Green Chemistry, 13 (2011)  
805 2561-2568.
- 806 [26] J.-S. Choi, G. Bugli, G. Djéga-Mariadassou, Influence of the Degree of  
807 Carburization on the Density of Sites and Hydrogenating Activity of Molybdenum  
808 Carbides, Journal of Catalysis, 193 (2000) 238-247.
- 809 [27] M.P. Vorob'eva, A.A. Greish, A.V. Ivanov, L.M. Kustov, Preparation of catalyst  
810 carriers on the basis of alumina supported on metallic gauzes, Applied Catalysis A:  
811 General, 199 (2000) 257-261.
- 812 [28] P. Gajardo, A. Mathieux, P. Grange, B. Delmon, Structure and catalytic activity of  
813 CoMo/γ-Al<sub>2</sub>O<sub>3</sub> and CoMo/SiO<sub>2</sub> hydrodesulphurization catalysts: an xps and esr  
814 characterization of sulfided used catalysts, Applied Catalysis, 3 (1982) 347-376.
- 815 [29] M. Hellinger, H.W.P. Carvalho, S. Baier, D. Wang, W. Kleist, J.-D. Grunwaldt,  
816 Catalytic hydrodeoxygenation of guaiacol over platinum supported on metal oxides and  
817 zeolites, Applied Catalysis A: General, 490 (2015) 181-192.

818 [30] A. Chambers, T. Nemes, N.M. Rodriguez, R.T.K. Baker, Catalytic behavior of  
819 graphite nanofiber supported nickel particles. 1. Comparison with other support media,  
820 Journal of Physical Chemistry B, 102 (1998) 2251-2258.

821 [31] C. Pham-Huu, N. Keller, G. Ehret, L.J. Charbonniere, R. Ziessel, M.J. Ledoux,  
822 Carbon nanofiber supported palladium catalyst for liquid-phase reactions - An active  
823 and selective catalyst for hydrogenation of cinnamaldehyde into hydrocinnamaldehyde,  
824 Journal of Molecular Catalysis a-Chemical, 170 (2001) 155-163.

825 [32] N.M. Rodriguez, M.S. Kim, R.T.K. Baker, CARBON NANOFIBERS - A  
826 UNIQUE CATALYST SUPPORT MEDIUM, Journal of Physical Chemistry, 98 (1994)  
827 13108-13111.

828 [33] J. Zhu, A. Holmen, D. Chen, Carbon Nanomaterials in Catalysis: Proton Affinity,  
829 Chemical and Electronic Properties, and their Catalytic Consequences, ChemCatChem,  
830 5 (2013) 378-401.

831 [34] G.-H. Liu, Z.-M. Zong, Z.-Q. Liu, F.-J. Liu, Y.-Y. Zhang, X.-Y. Wei, Solvent-  
832 controlled selective hydrodeoxygenation of bio-derived guaiacol to arenes or phenols  
833 over a biochar supported Co-doped MoO<sub>2</sub> catalyst, Fuel Processing Technology, 179  
834 (2018) 114-123.

835 [35] P. Serp, J.L. Figueiredo, Carbon Materials for Catalysis, 2008.

836 [36] J.S. Lee, S.T. Oyama, M. Boudart, Molybdenum carbide catalysts, J. Catal., 106  
837 (1987) 125-133.

838 [37] B. Frank, K. Friedel, F. Girgsdies, X. Huang, R. Schlögl, A. Trunschke, CNT-  
839 Supported MoxC Catalysts: Effect of Loading and Carburization Parameters,  
840 ChemCatChem, 5 (2013) 2296-2305.

841 [38] S.F. Hashmi, H. Meriö-Talvio, K.J. Hakonen, K. Ruuttunen, H. Sixta,  
842 Hydrothermolysis of organosolv lignin for the production of bio-oil rich in  
843 monoaromatic phenolic compounds, Fuel Processing Technology, 168 (2017) 74-83.

844 [39] A. Agarwal, M. Rana, J.-H. Park, Advancement in technologies for the  
845 depolymerization of lignin, Fuel Processing Technology, 181 (2018) 115-132.

846 [40] X. Lv, Q. Li, Z. Jiang, Y. Wang, J. Li, C. Hu, Structure characterization and  
847 pyrolysis behavior of organosolv lignin isolated from corncob residue, Journal of  
848 Analytical and Applied Pyrolysis, 136 (2018) 115-124.

849 [41] Y.-K. Hong, D.-W. Lee, H.-J. Eom, K.-Y. Lee, The catalytic activity of Pd/WO<sub>x</sub>/γ-  
850 Al<sub>2</sub>O<sub>3</sub> for hydrodeoxygenation of guaiacol, Applied Catalysis B: Environmental, 150-  
851 151 (2014) 438-445.

852 [42] Q. Lai, C. Zhang, J.H. Holles, Hydrodeoxygenation of guaiacol over Ni@Pd and  
853 Ni@Pt bimetallic overlayer catalysts, Applied Catalysis A: General, 528 (2016) 1-13.

854 [43] X. Lan, E.J.M. Hensen, T. Weber, Hydrodeoxygenation of guaiacol over  
855 Ni<sub>2</sub>P/SiO<sub>2</sub>-reaction mechanism and catalyst deactivation, Applied Catalysis A:  
856 General, 550 (2018) 57-66.

857 [44] E. Ochoa, D. Torres, R. Moreira, J.L. Pinilla, I. Suelves, Carbon nanofiber  
858 supported Mo<sub>2</sub>C catalysts for hydrodeoxygenation of guaiacol: The importance of the  
859 carburization process, Applied Catalysis B: Environmental, 239 (2018) 463-474.

860 [45] D. Raikwar, M. Munagala, S. Majumdar, D. Shee, Hydrodeoxygenation of  
861 guaiacol over Mo, W and Ta modified supported nickel catalysts, Catalysis Today,  
862 (2018).

863 [46] R. Moreira, E. Ochoa, J. Pinilla, A. Portugal, I. Suelves, Liquid-Phase  
864 Hydrodeoxygenation of Guaiacol over Mo<sub>2</sub>C Supported on Commercial CNF. Effects  
865 of Operating Conditions on Conversion and Product Selectivity, Catalysts, 8 (2018)  
866 127.

- 867 [47] A.L. Jongerius, R.W. Gosselink, J. Dijkstra, J.H. Bitter, P.C.A. Bruijninx, B.M.  
868 Weckhuysen, Carbon Nanofiber Supported Transition-Metal Carbide Catalysts for the  
869 Hydrodeoxygenation of Guaiacol, *ChemCatChem*, 5 (2013) 2964-2972.
- 870 [48] E. Santillan-Jimenez, M. Perdu, R. Pace, T. Morgan, M. Crocker, Activated  
871 Carbon, Carbon Nanofiber and Carbon Nanotube Supported Molybdenum Carbide  
872 Catalysts for the Hydrodeoxygenation of Guaiacol, *Catalysts*, 5 (2015) 424-441.
- 873 [49] T. Yang, L. Shi, R. Li, B. Li, X. Kai, Hydrodeoxygenation of crude bio-oil in situ  
874 in the bio-oil aqueous phase with addition of zero-valent aluminum, *Fuel Processing*  
875 *Technology*, 184 (2019) 65-72.
- 876 [50] C.-C. Tran, F. Stankovikj, M. Garcia-Perez, S. Kaliaguine, Unsupported transition  
877 metal-catalyzed hydrodeoxygenation of guaiacol, *Catalysis Communications*, 101  
878 (2017) 71-76.
- 879 [51] V.N. Bui, D. Laurenti, P. Afanasiev, C. Geantet, Hydrodeoxygenation of guaiacol  
880 with CoMo catalysts. Part I: Promoting effect of cobalt on HDO selectivity and activity,  
881 *Applied Catalysis B: Environmental*, 101 (2011) 239-245.
- 882 [52] H.Y. Cai, J.M. Shaw, K.H. Chung, The impact of solid additives on the apparent  
883 solubility of hydrogen in petroleum fractions and model hydrocarbon liquids, *Fuel*, 80  
884 (2001) 1065-1077.
- 885 [53] K.A. Rogers, Y. Zheng, Selective Deoxygenation of Biomass-Derived Bio-oils  
886 within Hydrogen-Modest Environments: A Review and New Insights, *ChemSusChem*,  
887 9 (2016) 1750-1772.
- 888 [54] A.N. Kay Lup, F. Abnisa, W.M.A.W. Daud, M.K. Aroua, A review on reaction  
889 mechanisms of metal-catalyzed deoxygenation process in bio-oil model compounds,  
890 *Applied Catalysis A: General*, 541 (2017) 87-106.

891